Talanta 85 (2011) 104–111

Contents lists available at ScienceDirect

Talanta

journal homepage: www.elsevier.com/locate/talanta

In situ chemo-synthesized multi-wall carbon nanotube-conductive polyaniline nanocomposites: Characterization and application for a glucose amperometric biosensor

Huaan Zhong, Ruo Yuan*, Yaqin Chai, Wenjuan Li, Xia Zhong, Yu Zhang

Education Ministry Key Laboratory on Luminescence and Real-Time Analysis, College of Chemistry and Chemical Engineering, Southwest University, Chongqing 400715, People's Republic of China

ARTICLE INFO

Article history:
Received 21 January 2011
Received in revised form 11 March 2011
Accepted 17 March 2011
Available online 30 March 2011

Keywords:
Polyaniline
Multi-wall carbon nanotube
Biosensor
Platinum nanoparticles
Glucose oxidase
Composites

ABSTRACT

A new glucose amperometric biosensor, based on electrodeposition of platinum nanoparticles onto the surface of multi-wall carbon nanotube (MWNT)-polyaniline (PANI) nanocomposites, and then immobilizing glucose oxidase (GOD) with covalent interaction and adsorption effect, was constructed in this paper. Firstly, the MWNT-PANI nanocomposites had been synthesized by in situ polymerization and were characterized through transmission electron microscopy (TEM), Fourier transform infrared (FT-IR) spectroscopy, and ultraviolet and visible (UV–vis) absorption spectra. The assembled process of the modified electrode was probed by scanning electron microscopy (SEM) and cyclic voltammetry (CV). Chronoamperometry was used to study the electrochemical performance of the resulting biosensor. The glucose biosensor exhibited a linear calibration curve over the range from 3.0 μM to 8.2 mM, with a detection limit of 1.0 μM and a high sensitivity of 16.1 μA mM^{-1}. The biosensor also showed a short response time (within 5 s). Furthermore, the reproducibility, stability and interferences of the biosensor were also investigated.

1. Introduction

The development of a glucose biosensor is significant due to the prevalence of diabetes mellitus as a major health threat in the world. The normal value of the blood glucose concentration in a healthy adult serum is 80–120 mg/dL (4.4–4.6 mM), which is an important parameter for the diagnosis and prevention of disease [1]. Since Clark and Lyons proposed the initial concept of glucose enzyme electrodes in 1962 [2], an enormous number of various glucose biosensors have been represented a very active area in biosensor research [3–16]. The amperometric biosensor is chosen for biochemical analysis because of its rapid response, good selectivity, and low cost [3–5,7–16]. In recent years, to improve the sensitive of glucose biosensor, nanomaterials have received great attention because of their unique electronic, chemical and mechanical properties. Materials like metal (gold, silver, platinum), metal oxide (ZnO, Fe_2O_3, CuO_2), carbon and polymers (especially conducting polymers: polypyrrole, polyaniline, polythiophene) have been used to prepare nanomaterials such as nanoparticles [9–11], nanotubes [10,12], nanowires [13,14] and nanofibres [15,16].

Polyaniline (PANI), which was discovered over about 150 years, is unique among the class of conducting polymers. Generally, there are three redox forms of PANI: pernigraniline (PG), leucoemeraldine (LE) and emeraldine. PG is fully oxidized state with imine links instead of amine links. LE is fully reduced state. PG and LE are poor conductors, even when doped with acid. The emeraldine form of PANI, usually referred to as emeraldine base (EB), is either neutral or doped, with imine nitrogens protonated by an acid. Doping and depoing with acid and base can interchange EB and emeraldine salt forms of PANI. EB is regarded as the most useful form of PANI due to its high stability at room temperature and moreover its doped form is electrically conducting [17,18]. Recently, PANI has captured attention of researchers due to its polymer chain structure with high conductivity, environmental stability and low cost [18,19]. This conducting polymer might be greatly applied in many biosensors in virtue of its especial properties such as: (i) high surface area and chemical specificities, (ii) redox conductivity and polyelectrolyte characteristics, (iii) direct and easy deposition on the electrode. Moreover, its electrical properties can be reversibly controlled by both charge-transfer doping and protonation.

Carbon nanotube (CNT) has emerged a wealth of exceptional electrical, mechanical and thermal properties, which have made them useful for potential application ranging from nanoelectronics to biomedical devices [20]. Recently, composite materials based on integration of CNT and some materials to possess properties of

* Corresponding author. Tel.: +86 23 68252277; fax: +86 23 68253172.
E-mail address: yuanruo@swu.edu.cn (R. Yuan).

0039-9140/$ – see front matter © 2011 Elsevier B.V. All rights reserved.
doi:10.1016/j.talanta.2011.03.040

the individual components with a synergistic effect have gained growing interest. Materials for such purposes contain conducting polymers, redox mediators and metal nanoparticles. Thereinto, CNT/polymer nanocomposites have been pursued with the hope of delivering CNT properties to a processable and synergistic host [21–26]. Many polymers have been used as matrix materials in CNT/polymer composites for various target applications. For example, CNT was used as a conductive filler for CNT/poly (3-octylthiophene) composites, and CNT/poly (phenylenevinylene) composites have also been reported [22,23]. To date, it has been reported that the CNT/PANI composites exhibited an order of magnitude increase in electrical conductivity over neat PANI [25,26]. Other reports have shown that aniline itself can interact strongly with CNT via donor–acceptor interactions as evidenced by the relatively high solubility of CNT in aniline [27]. Feng et al. have successfully synthesized MWNT-PANI composite films by in situ polymerization with ammonium peroxidisulfate, and found to be orientationally ordered by the aligned MWNT [28]. However, there is no report on the synthesis of MWNT-PANI nanocomposites in acidic solution by in situ polymerization with potassium persulfate (KPS) as oxidant in the presence of MWNT and using it to immobilization of protein molecules for biosensor fabrication.

In the present work, a new glucose biosensor was constructed based on MWNT-PANI nanocomposite films which formed during a chemically oxidative process in situ polymerization of aniline with KPS as oxidant in the presence of MWNT in sulfuric acid solution. Firstly, MWNT-PANI nanocomposites were immobilized on a glassy carbon electrode (GCE) surface to obtain conductive, redox and porous nanostructured film. Subsequently, Pt nanoparticles were deposited on the MWNT-PANI nanocomposites by potentiometric stripping analysis method. Finally, GOD was adsorbed on the surface of Pt/MWNT-PANI film via covalent interaction with glutaraldehyde (GA) and adsorption effect with Pt nanoparticles. The MWNI-PANI nanocomposites were characterized by transmission electron microscopy (TEM), Fourier tansform infrared (FT-IR) spectroscopy, and ultraviolet and visible (UV–vis) absorption spectra. The electrode modification process was probed by scanning electron microscopy (SEM) and cyclic voltammetry (CV), and the optimization of the experimental conditions and the performance of the glucose biosensor were studied by chronoamperometry in details.

2. Experiment

2.1. Reagent and materials

Aniline, chloroplatinic acid ($H_2PtCl_6{\cdot}6H_2O$), and glucose oxidase (GOD, EC 1.1.3.4, 151,000 units/g), multi-wall carbon nanotube (MWNT) were obtained from Sigma Chemical Co. (St. Louis, MO, USA). 25% glutaraldehyde (GA) water solution, potassium persulfate (KPS; $K_2S_2O_8$), and glucose were purchased from Shanghai Chemical Reagent Co. (Shanghai, China). Glucose stock solutions were allowed to mutarotate overnight at room temperature before use. Purified aniline was obtained by distilling several times until a colorless liquid was observed. Phosphate buffer solutions (PBS) with various pH values were prepared with stock standard solutions (containing 0.9% NaCl) of 0.1 M KH_2PO_4 and 0.1 M Na_2HPO_4. All of the other chemicals were analytical grade. Twice-distilled water was used throughout.

2.2. Apparatus

Ultraviolet and visible (UV–vis) absorption spectra were carried out on a Lambda 17 UV–vis 8500 spectrometer (PE Co., USA) with quartz cuvette (pathlength 1 cm). Fourier transform infrared spectroscopy (FT-IR) measurement of the composite was carried out on a Jasco FT/IR-300E instrument (Jasco Ltd., Tokyo, Japan). Transmission electron microscopy (TEM) was obtained by using a H600 TEM (Hitachi, Tokyo, Japan). Scanning electron microscopy (SEM) images were recorded with an S-4800 SEM (Hitachi, Tokyo, Japan). Cyclic voltammetric and amperometric measurements were performed using a CHI 660D electrochemical station (CH Instruments, Chenhua Corp., Shanghai, China) at room temperature. All experiments were carried out using a conventional three-electrode system with a bare or modified glassy carbon electrode (GCE) (Φ = 4 mm) as a working electrode, a platinum wire as an auxiliary electrode, and a saturated calomel electrode (SCE) as a reference electrode. The test solutions were 5 mL PBS solutions, which were deoxygenated by bubbling highly pure nitrogen for 20 min before electrochemical experiments, and maintained under nitrogen atmosphere during measurements.

2.3. Synthesis of MWNT-conductive PANI nanocomposites

The MWNT were purified as reported previously [29]. Briefly, 50 mg of MWNT oxidized at 300 °C for 6 h to remove amorphous carbon particles. To eliminate metal oxide catalysts, the oxidized MWNT were dispersed in 25 mL of 6.0 mol/L HCl for 2 h under ultrasonic agitation, washed until the pH of the solution was near to neutral, and then dried in a vacuum oven at 80 °C for 8 h.

MWNT-conductive PANI nanocomposites were prepared according to the following steps: 68.8 μL of freshly distilled aniline was dissolved in 5 mL of 0.5 mol/L H_2SO_4 solution and the whole of aniline solution was added in several portions with constant stirring. Then 2.0 mg the purification of MWNT were dipped in the aniline/H_2SO_4 solution for 12 h, which led to the adsorption aniline monomer on the nanotubes. Later, 5.0 mL solution of KPS (0.15 mol/L) was added dropwise under vigorous stirring. The polymerization reaction was carried out at 0 °C for 6 h. In this process the color of the solution changed from transparent to pale green, and finally changed to deep green. The MWNT-PANI nanocomposites were centrifuged, washed in double-distilled water and ethanol, respectively. As compare, the pure PANI was prepared at the same condition without MWNT.

2.4. Preparation of the glucose biosensors

The glassy carbon electrode was polished successively with 0.3 and 0.05 μm Al_2O_3 before modification, rinsed with double-distilled water thoroughly, and ultrasonically cleaned in acetone and double-distilled water for 5 min, respectively.

The stepwise procedure of the glucose biosensor and the reaction occurring at surface of the GOD-modified electrode during determination of glucose are illustrated in Scheme 1. Firstly, 1.0 mg MWNT-PANI nanocomposites were dispersed in 1.0 mL doubly distilled water. Then 10 μL of the mixed suspension was coated on the surface of cleaned GCE and dried in the air (Scheme 1a). Subsequently, Pt nanoparticles were electrodeposited on the nanocomposites film for 100 s at −0.2 V in 19.3 mmol/L H_2PtCl_6 solution (Scheme 1b). After that, a mixture was prepared by adding GOD and GA in 0.1 M PBS (pH 7.0). The concentration of enzyme and GA was 2.5 mg/mL and 0.25% (V/V), respectively. Finally, 5 μL of the mixture solution was dropped on the surface of the Pt/MWNT-PANI nanocomposites modified electrode and allowed todry for 8 h

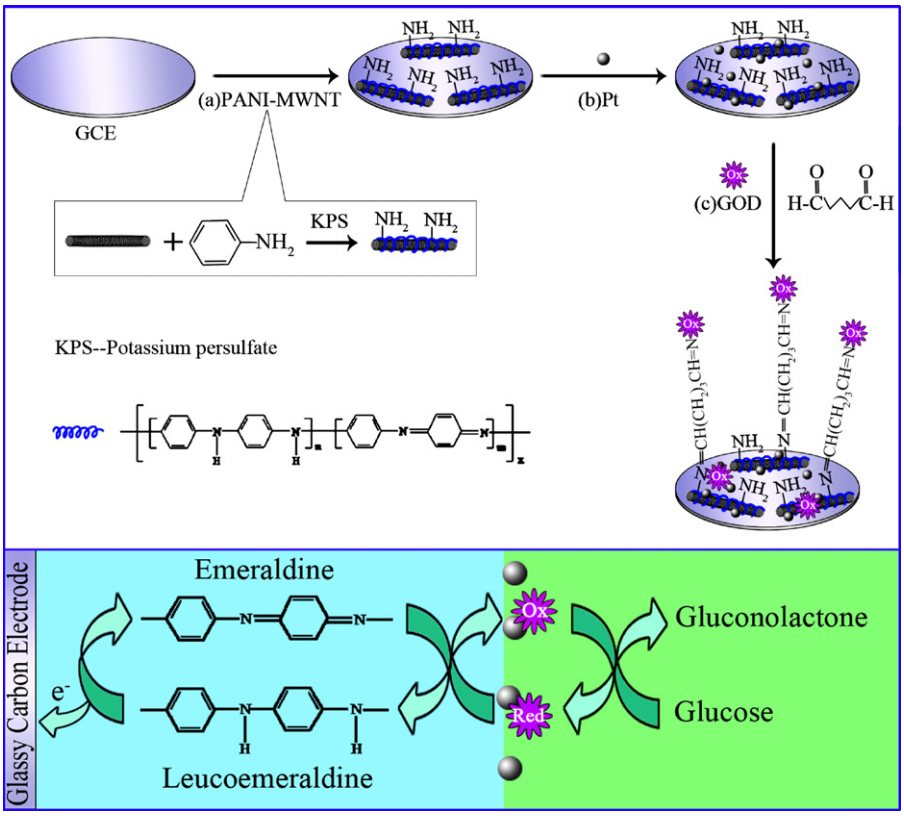

Scheme 1. Illustration of the preparation process of glucose biosensor and the reaction occurring at surface of the GOD-modified electrode during determination of glucose.

at 4 °C (Scheme 1c). When not in use, the fabricated biosensor was stored in 0.1 M PBS at 4 °C.

3. Results and discussion

3.1. Characterizations of the MWNT-PANI nanocomposites by TEM, FT-IR and UV–vis

To confirm into the structural features of the MWNT-PANI nanocomposites, TEM was applied to study its surface morphology. For comparison, a TEM image of the original MWNT was shown in Fig. 1. Fig. 1a showed clearly that the tubular structure of MWNT having diameters of around 15 nm. From Fig. 1b, obviously increase in the diameter of MWNT after the MWNT-PANI nanocomposites formation reveals wrapping of MWNT with PANI. The composites with diameters about 25 nm were also clearly found in the sample, indicating that PANI could be loaded onto the surface of MWNT and relatively uniform inorganic–organic nanocomposites were formed.

Fig. 2 showed the FT-IR spectra of PANI and MWNT-PANI nanocomposites. The PANI polymer displayed the characteristic bands of secondary amine (N–H) at 3230 cm^{-1}, the C=C stretching deformation of the quinoid at 1568 cm^{-1}, benzenoid rings at 1501 cm^{-1}, and the C–N stretching of the secondary aromatic amine at 1289 cm^{-1}, the C–H (out-of-plane) of stretching of the p-disubstituted benzene ring at 824 cm^{-1} (Fig. 2a). The MWNT-PANI nanocomposites displayed almost identical characteristic bands at 3135, 1581, 1497, and 1305, 821 cm^{-1} (Fig. 2b), respectively, which were in accordance with the previous reports [28,30]. This proved that the MWNT-PANI nanocomposites had been successfully synthesized by in situ polymerization.

UV–vis absorption was conducted to study the interfacial interaction between PANI and MWNT. Stock solution (10 mg/mL) of

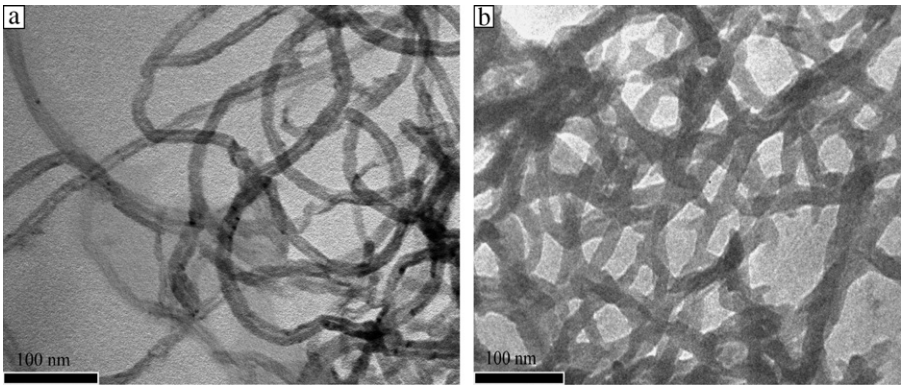

Fig. 1. TEM image of the purified MWNTs (a), the obtained MWNT-PANI nanocomposites (b).

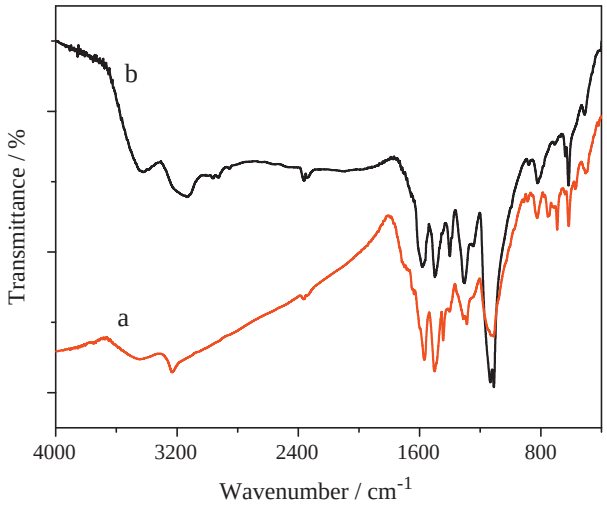

Fig. 2. FT-IR (KBr pellet) spectra: PANI (a), MWNT-PANI nanocomposites (b).

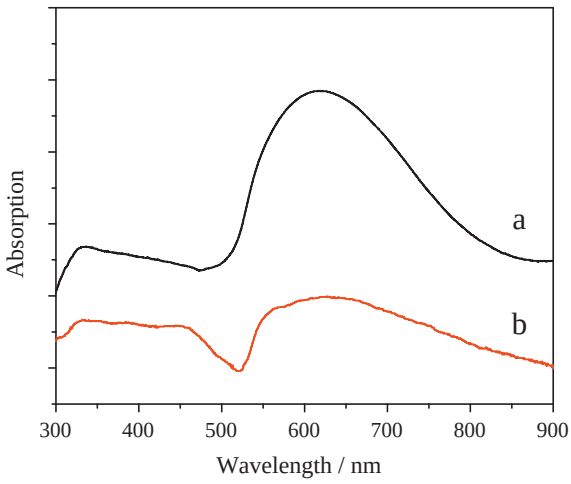

Fig. 3. UV–vis absorption spectra of PANI (a), MWNT-PANI nanocomposites (b).

each sample was prepared in water. The UV–vis absorption of PANI showed two peaks at 323 and 611 nm (Fig. 3a). Both peaks are related to the $\pi \rightarrow \pi^*$ transition of benzenoid ring and quinoid ring in PANI, respectively [31,32]. Compared to the PANI polymer, the peaks from MWNT-PANI red-shifted by 5 and 19 nm and showed maxima at 328 and 630 nm (Fig. 3b), respectively. This implies that there was a strong interaction between PANI and MWNT, and PANI was covalently grafted and physically absorbed onto the surface of MWNT.

3.2. Scanning electron microscope of the modification process of biosensor

The SEM was used to present the morphologies and microstructures of the as-prepared different modified films (Fig. 4). Fig. 4a showed an image of the GCE surface coated with MWNT-PANI nanocomposites layer, obviously, the porous MWNT-PANI modified electrode had larger surface compared with the ordinary GCE. From Fig. 4b, when platinum were electrodeposited on to the surface of modified electrode, some of Pt nanoparticles were modified on the surface of MWNT-PANI, and the others could be seen

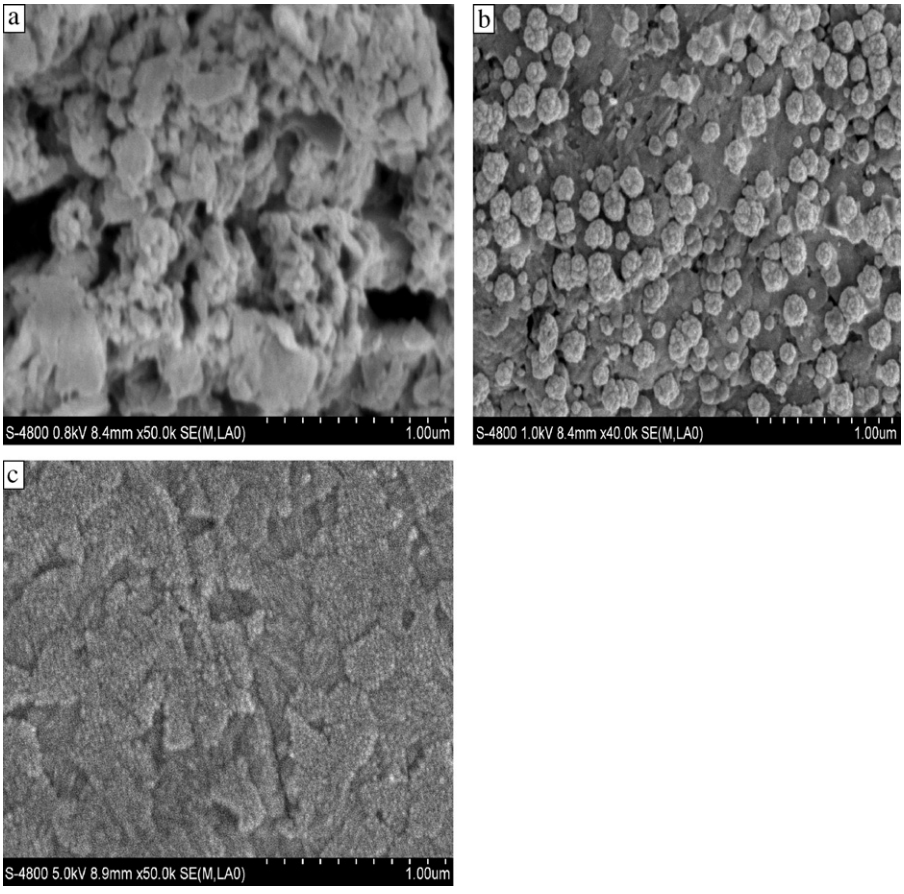

Fig. 4. SEM of different nanocomposite films: MWNT-PANI (a), Pt/MWNT-PANI (b), and GOD/Pt/MWNT-PANI (c).

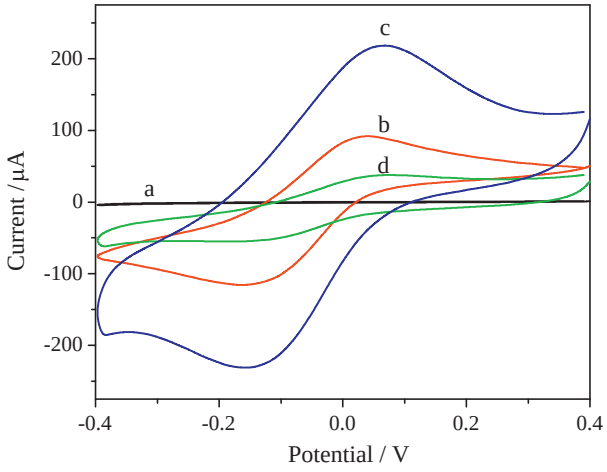

Fig. 5. Cyclic voltammetry of the bare glassy carbon electrode (a), MWNT-PANI/GCE (b), Pt/MWNT-PANI/GCE (c), and GOD/Pt/MWNT-PANI/GCE (d) in 0.1 M PBS (pH 7.0) at a scan rate of 50 mV/s.

that they were filled the interspaces of nanocomposites. As shown in Fig. 4c, when GOD was immobilized on Pt/MWNT-PANI/GCE, the corresponding SEM image obviously changed. This revealed that the Pt/MWNT-PANI layer with large specific surface area and good biocompatibility could load more protein without losing their bioactivities. On the basis of SEM results, we concluded that the fabricated biosensor could preliminarily be applied for detection of glucose.

3.3. Cyclic voltammetric behavior of modified electrode

The cyclic voltammetric experiments were conducted to further characterize the stepwise assembly of the glucose biosensors. As shown in Fig. 5, the CVs of differently modified electrodes were given in the potential range of −0.4 to 0.4 V in PBS (pH 7.0) with a scan rate of 50 mV/s. No redox waves could be observed on a bare GCE (Fig. 5a) because of the lack of substance with electrochemical activity. When the electrode was coated with MWNT-conductive PANI nanocomposites, a well-defined redox peak at 0.04 and 0.16 V vs. SCE (Fig. 5b) could be found. It was the reason that MWNT-PANI composites were an excellent redox-active material attributed to the redox of the PANI form emeraldine state to leucoemeraldine (LE) [33]. After electrodeposite Pt nanoparticles onto the surface of a MWNT-PANI/GCE (Fig. 5c), the anodic and cathodic peaks current increased, because the conductive Pt nanoparticles could accelerate the reaction of PANI. The current peak obviously decreased after GOD were immobilized onto the Pt/MWNT-PANI/GCE (Fig. 5d), which was attributed to the fact that GOD insulated the conductive support and hindered the transfer of electrons toward electrode surface. CV responses of the biosensor at different scan rates were investigated in PBS (pH 7). The result showed that the peak current increased with the scan rates in range of 5–600 mV/s (Fig. 6A). Square root of scan rate showed a linear relation with peak current (Fig. 6B), indicting a diffusion-controlled process of the biosensor.

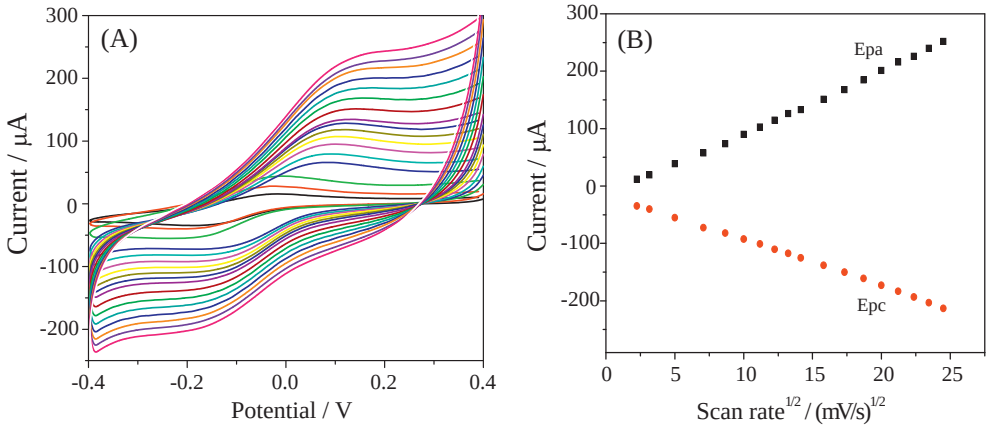

Fig. 6. Cyclic voltammetry of the biosensor at different scan rates (from inner to outer): 5, 10, 25, 50, 75, 100, 125, 150, 175, 200, 250, 300, 400, 450, 500, 550 and 600 mV/s in 5 mL 0.1 M PBS (pH 7.0) under room temperature (A), and the redox peak currents versus $V^{1/2}$ (B).

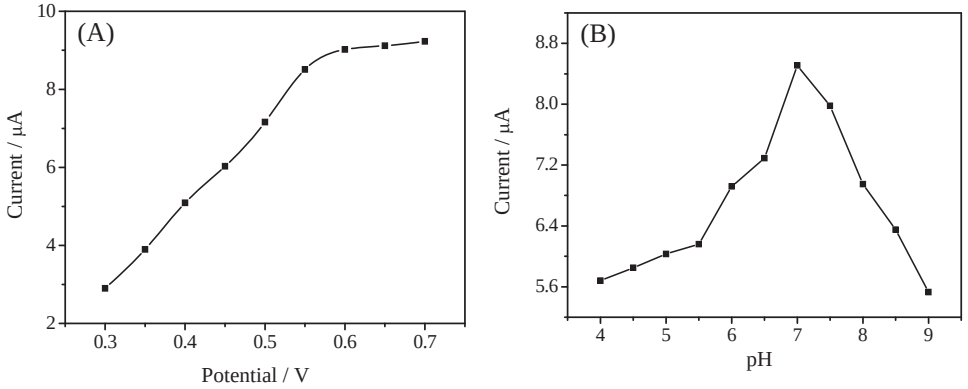

Fig. 7. Dependence of the current change of biosensor to 0.6 mM glucose on the applied potential in 0.1 M PBS (pH 7.0) (A), and the pH of PBS (0.1 M) at an applied potential of 0.55 V (B).

3.4. Optimization of the experimental conditions

To improve the analytical characteristics of the biosensor, optimization of experimental conditions for the glucose biosensor was carried out in terms of pH and applied potential in amperometry.

3.4.1. Influence of applied potential

The effect of applied potential on the amperometric current response was studied for the GOD/Pt/MWNT-PANI/GCE (Fig. 7A). As shown, the current response increased as the applied potential shifted from 0.30 to 0.70 V. The response current increases rapidly when the potential was moved from 0.30 to 0.55 V. However, when the potential was further shifted to the positive direction, the response current increased very slowly. Withal, the high operating potential results in interference from the matrix species. Therefore, 0.55 V was chosen as the optimum applied potential for further study.

3.4.2. Influence of pH value

As is well known, the pH value of the electrolyte is important for the performance of the biosensor because the activity of the enzyme is affected greatly by pH of the solution. Fig. 7B showed the correlation between the response currents and the pH values (4.0–9.0). The current increased with increasing pH of the solution until it reached 7.0. But the further increases in the pH decreased the current response. So a PBS of pH 7.0 was selected for glucose detection in this study.

3.5. Amperometric response of the glucose biosensor

Electrocatalytic activity of the GOD/Pt/MWNT-PANI/GCE for glucose was estimated by CV (Fig. 8). With the increase of glucose concentration, the oxidation peak current increased with the decrease of the reduction peak current, which indicated that enzyme molecules were immobilized on the surface of modified electrode successfully.

In order to check up the electrochemical response of the modified biosensor, comparative studies of the amperometric responses were carried out by using different modified electrodes for continuous addition of glucose to a continuously stirred 5 mL PBS (pH 7.0) solution at applied potential of 0.55 V. Fig. 9 showed current–time curves of GOD/Pt/MWNT-PANI/GCE (a), GOD/Pt/GCE (b) and GOD/MWNT-PANI/GCE (c). From the current–time curves, we could see the target electrode (a) showed the best response to addition of the same glucose concentration under the optimized conditions, which attributed to the synergistic electro-catalytic

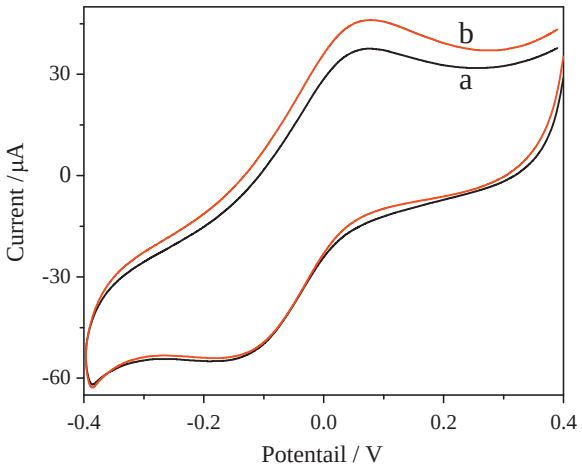

Fig. 8. Cyclic voltammetry of enzyme electrode in 0.1 M PBS (pH 7.0) without glucose (a) and with 0.6 mM glucose (b).

activity between Pt nanoparticles and MWNT-PANI nanocomposites.

The amperometric response of the glucose biosensor was investigated under the optimized conditions. The typical current–time curve of the biosensor was shown in Fig. 10. The response current of the biosensor increased with the increasing of glucose. The biosensor showed fast response achieving 95% of the steady-state current within 5 s. The response current increased linearly with the glucose concentration in the range of 3.0 μM to 8.2 mM with a correlation coefficient of 0.9989 ($n = 22$) (the lower inset of in Fig. 10). From the slope of the calibration curve, the detection limit of 1.0 μM was estimated at a signal-to-noise ratio of three. The sensitivity for glucose determination was about 16.1 μA mM^{-1}. The performance of the GOD/Pt/MWNT-PANI biosensor developed in this study was compared with other glucose biosensors as listed in Table 1. This reveals that our proposed biosensor shows excellent performance in terms of low detection limit, long linear range and high sensitivity.

The apparent Michaelis-Menten constant (K_M^{app}) is a reflection of both the enzymatic affinity and the ratio of microscopic kinetic constant. When the concentration of glucose was higher than 8.2 mM, the response of the glucose biosensor deviated from the straight line and reached a plateau (the lower inset of in Fig. 10), which were the characteristics of Michaelis-Menten kinetics. The K_M^{app} can be calculated according to the Lineweaver-Burk equation [42]:

$$\frac{1}{i_{ss}} = \frac{1}{i_{max}} + \frac{K_M^{app}}{i_{max} \times c}$$

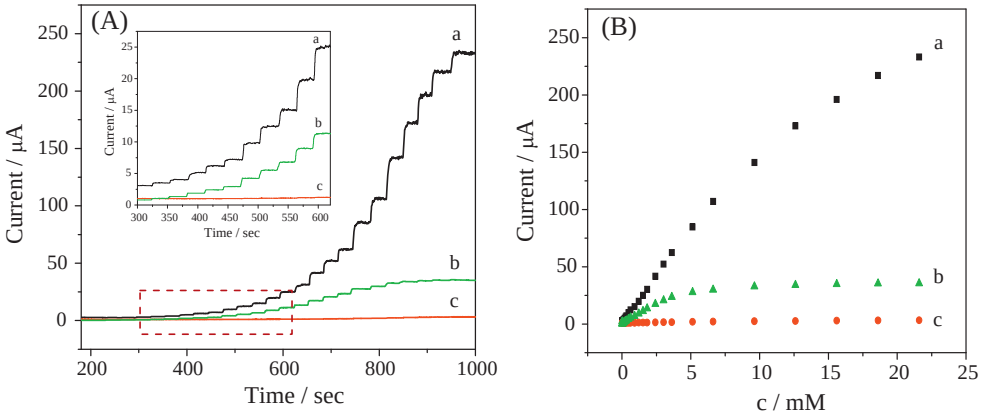

Fig. 9. Amperometric response (A) and the calibration curve of glucose (B) of GOD/Pt/MWNT-PANI/GCE (a), GOD/Pt/GCE (b), and GOD/MWNT-PANI/GCE (c) in a stirred 0.1 M PBS (pH 7.0) after successive glucose additions at applied potential of 0.55 V. Inset shows a magnification of the 300–620 s additions of glucose.

Table 1
Comparison of performances of proposal biosensor for glucose detection with those of biosensors based on different matrices.

Modified electrode	Linear range (mM)	Detection limit (μM)	Sensitivity (μA mM^{-1})	Applied potential (V) (vs. SCE)	R^2	Reference
GOD/Pt/MWNT-PANI/GCE	0.003–8.2	1.0	16.1	0.55	0.9989 (n = 22)	This work
{GOx/Au-(SH)PANI-g-MWNT}$_n$/ITO	1–9	0.06	3.97	0.40 vs. Ag/AgCl	0.998 (n = 9)	[34]
GOD/CS-CNTs/PANI/Au	1–20	100	16.5	0.50 vs. Ag/AgCl	–	[35]
GOx/PANI-g-MWNT/Nafion-silica/ITO	1–10	0.01	5.01	0.20 vs. Ag/AgCl	0.9992 (n = 9)	[36]
Au-PANI/GOD/Nafion/GCE	0.001–0.8	0.5	2.3	0.60	0.999 (n = 9)	[37]
GOD/Pt-SWCNTs/GCE	0.0005–5	0.5	2.11	0.55 vs. Ag/AgCl	0.998 (n = 7)	[10]
GOD-Chitosan-SiO$_2$/Pt/MWNTs/GCE	0.001–23	1.0	–	0.60	0.999 (n = 23)	[38]
GOx-nanoPANI/Pt	0.01–5.5	0.3 ± 0.1	7.58 ± 0.36	−0.30	0.996	[39]
GOD/MWNT-Nafion/GCE	0.05–2	4	0.33	0.70 vs. Ag/AgCl	0.999	[40]
Pt/CMK-3-GOx-gelatin/GCE	0.04–12.2	1	–	0.60	0.996 (n = 10)	[41]

Where i_{ss} is the steady-state current after the addition of substrate; i_{max} is the maximum current measured under saturated substrate condition; c is the bulk concentration of the substrate. The value of K_M^{app} was estimated to be 0.64 mM. It was lower than the value of either previous report for the PMPD-GOD/Pt/PANI modified electrode (K_M^{app} = 9.34 mM) [16], the TTF/hybrid-GOx/Nafion modified electrode (K_M^{app} = 22.0 mM) [5] and POAP-GOD/PPy-Pt/GCE (K_M^{app} = 23.9 mM) [43]. This result suggested that GOD immobilized in Pt/MWNT-PANI nanocomposite films retained its biological activity and had a high biological affinity to glucose.

3.6. Reproducibility, stability, and interference of the glucose biosensor

The biosensor reproducibility was investigated from the response for 0.60 mM glucose at eight different electrodes, which showed good reproducibility for the determination of glucose concentration in its linear range. The relative standard deviation (RSD) was 4.3%. The storage stability of the biosensor was also examined. When the biosensor was stored at 4 °C and measured intermittently (every 3 days), after 48 days of storage, the biosensor retained about 90% of its initial response. This good reproducibility and stability may be owed to the GOD molecules were stably immobilized on the Pt/MWNT-PANI membrane which provided a good biocompatible microenvironment.

In addition, the potential interference of some biological substance was investigated. In our experiments, the test solutions were deaerated by high pure nitrogen. The interference experiments were performed in PBS under optimum conditions by comparing the current response to 0.60 mM glucose in the presence of 1.00 mM of each interfering substance (uric acid, ethanol, L-cysteine, ascorbic acid, and L-tyrosine) with that to 0.60 mM glucose alone. They are 1.09 for uric acid, 0.98 for ethanol, 0.93 for L-cysteine, 0.98 for ascorbic acid and 1.04 for L-tyrosine. The results of the interference study showed that five interfering substances did not cause observable interference.

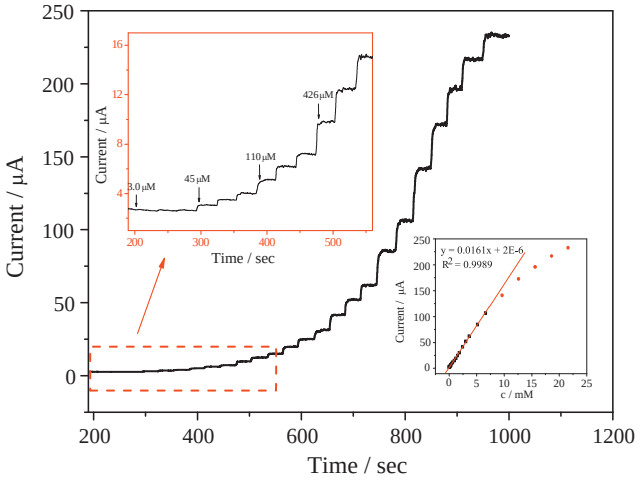

Fig. 10. Typical current–time response current of the biosensor upon successive adding different concentrations of glucose into a stirred solution of 0.1 M PBS (pH 7.0) at applied potential of 0.55 V. Inset shows the linear calibration curve.

Table 2
Determination of glucose in human serum samples.

Samples no.	Determined by biosensor (mM)[a]	Measured by local hospital (mM)	R.S.D (%)
1	5.32	5.59	4.83
2	3.57	3.64	1.92
3	6.85	7.01	2.28

[a] Average of three measurements.

3.7. Glucose determination in serum samples

The analytical applicability of the biosensor was evaluated by determining of glucose in human serum samples. The sample was diluted 100 times with 0.1 M PBS at pH 7.0. The diluted samples were then analyzed by the prepared biosensor at a potential of 0.55 V. The results are shown in Table 2. As can be seen, the values measured by the proposed are very close to results obtained by the clinic determination in local hospital. It implies that the sensing ability of the proposed biosensor is not limited to glucose solution. It also can be used to test on human serum sample.

4. Conclusion

We have proposed preparation of the MWNT-PANI nanocomposite films by in situ polymerization with large specific surface, high conductivity, redox electrochemical activity and environmental stability. The resulting MWNT-PANI nanocomposites were followed by fabrication of a new glucose biosensor. Because of the synergistic catalytic activity between MWNT-PANI nanocomposites and Pt nanoparticles, the fabricated amperometric biosensor displayed high sensitive detection of glucose. It is expected that this technique of biosensor fabrication is potentially useful for glucose sensing in vitro or in vivo.

Acknowledgments

This work was supported by the National Natural Science Foundation of China (21075100), the Ministry of Education of China (project 708073), the Natural Science Foundation of Chongqing City (CSTC-2009BA1003), the 211 Project of Southwest University (the Third Term), China and High Technology Project Foundation of Southwest University (XSGX 02), China.

References

[1] J. Wang, Chem. Rev. 108 (2008) 814.
[2] L. Clark Jr., C. Lyons, Ann. N.Y. Acad. Sci. 102 (1962) 29.
[3] J. Gonzalo-Ruiz, M.A. Alonso-Lomillo, F.J. Muñnoz, Biosens. Bioelectron. 22 (2007) 1517.
[4] P.A. Fiorito, C.M.A. Brett, S.I. Córdoba de Torresi, Talanta 69 (2006) 403.
[5] B.Q. Wang, B. Li, Q. Deng, S.J. Dong, Anal. Chem. 70 (1998) 3170.
[6] G. Chang, Y. Tatsu, T. Goto, H. Imaishi, K. Morigaki, Talanta 83 (2010) 61.
[7] J. Kulys, H.E. Hansen, Biosens. Bioelectron. 9 (1994) 491.
[8] P.D. Hale, L.I. Boguslavsky, T. Inagaki, H.I. Karan, H.S. Lee, T.A. Skotheim, Y. Okamoto, Anal. Chem. 63 (1991) 677.
[9] W.J. Li, R. Yuan, Y.Q. Chai, Talanta 82 (2010) 367.
[10] S. Hrapovic, Y.L. Liu, K.B. Male, J.H.T. Luong, Anal. Chem. 76 (2004) 1083.
[11] T.T. Baby, S. Ramaprabhu, Talanta 80 (2010) 2016.
[12] Y.H. Lin, F. Lu, Z.F. Ren, Nano Lett. 4 (2004) 191.
[13] H.C. Wang, X.S. Wang, X.Q. Zhang, X. Qin, Z.X. Zhao, Z.Y. Miao, N. Huang, Q. Chen, Biosens. Bioelectron. 25 (2009) 142.
[14] S.M. Usman Ali, O. Nura, M. Willander, B. Danielsson, Sens. Actuators B 145 (2010) 869.
[15] M. Singh, P.K. Kathuroju, N. Jampana, Sens. Actuators B 143 (2009) 430.
[16] H.H. Zhou, H. Chen, S.L. Luo, J.H. Chen, W.Z. Wei, Y.F. Kuang, Biosens. Bioelectron. 20 (2005) 1305.
[17] G. Premamoy, K.S. Samir, C. Amit, Eur. Polym. J. 35 (1999) 699.
[18] C. Dhand, M. Das, M. Datta, B.D. Malhotra, Biosens. Bioelectron. 26 (2011) 2811.
[19] Rajesh, T. Ahuja, D. Kumar, Sens. Actuators B 136 (2009) 275.
[20] M.A. Dresselhaus, M. Ebdo, Top. Appl. Phys. 80 (2001) 11.
[21] Z.J. Zia, Z.Y. Wang, C.L. Xu, J. Liang, B.Q. Wei, D.H. Wu, S.W. Zhu, Mater. Sci. Eng. A 271 (1999) 395.
[22] I. Musa, M. Baxendale, G.A.J. Amaratunga, W. Eccleston, Synth. Met. 102 (1999) 1250.
[23] J.N. Coleman, S. Curran, A.B. Dalton, A.P. Davey, B. McCarthy, W. Blau, R.C. Barklie, Synth. Met. 102 (1999) 1174.
[24] H.S. Woo, R. Czerw, S. Webster, D.L. Carroll, J.W. Park, J.H. Lee, Synth. Met. 116 (1999) 369.
[25] M. Cochet, W.K. Maser, A.M. Benito, M.A. Callejas, M.T. Martinez, J.M. Benoit, J. Schreiber, O. chauvet, Chem. Commun. (2001) 1450.
[26] H. Zengin, W. Zhou, J. Jin, R. Czerw, D.W. Smith Jr., L. Echegoyen, D.L. Carroll, S.H. Foulger, J. Ballato, Adv. Mater. 14 (2002) 1480.
[27] Y. Sun, S.R. Wilson, D.I. Schuster, J. Am. Chem. Soc. 123 (2001) 5348.
[28] W. Feng, X.D. Bai, Y.Q. Lian, J. Liang, X.G. Wang, K. Yoshino, Carbon 41 (2003) 1551.
[29] N. Rajalakshmi, K.S. Dhathathreyan, A. Govindaraj, B.C. Satishkumar, Electrochim. Acta 45 (2000) 4511.
[30] I.Y. Jeon, S.W. Kang, L.S. Tan, J.B. Baek, J. Polym. Sci. Polym. Chem. 48 (2010) 3103.
[31] J.X. Huang, S. Virji, B.H. Weiller, R.B. Kaner, J. Am. Chem. Soc. 125 (2003) 314.
[32] A.I. Gopalan, K.P. Lee, P. Santhosh, K.S. Kim, Y.C. Nho, Compos. Sci. Technol. 67 (2007) 900.
[33] T. Trung, T.H. Trung, H. Chang-Sik, Electrochim. Acta 51 (2005) 984.
[34] S. Komathia, A.I. Gopalana, K.P. Lee, Biosens. Bioelectron. 24 (2009) 3131.
[35] D. Wan, S.J. Yuan, G.L. Li, K.G. Neoh, E.T. Kang, Appl. Mater. Interfaces 2 (2010) 3083.
[36] A.I. Gopalan, K.P. Lee, D. Ragupathy, S.H. Lee, J.W. Lee, Biomaterials 30 (2009) 5999.
[37] Y.Z. Xian, Y. Hu, F. Liu, Y. Xian, H.T. Wang, L.T. Jin, Biosens. Bioelectron. 21 (2006) 1996.
[38] Y.J. Zou, C.L. Xiang, L.X. Sun, F. Xu, Biosens. Bioelectron. 23 (2008) 1010.
[39] Z.Y. Wang, S.N. Liu, P. Wu, C.X. Cai, Anal. Chem. 81 (2009) 1638.
[40] Y.C. Tsai, S.C. Li, J.M. Chen, Langmuir 21 (2005) 3653.
[41] J.J. Yu, D.L. Yu, T. Zhao, B.Z. Zeng, Talanta 74 (2008) 1586.
[42] R.A. Kamin, G.S. Wilson, Anal. Chem. 52 (1980) 1198.
[43] J. Li, X.Q. Lin, Biosens. Bioelectron. 22 (2007) 2898.